AIAA JOURNAL
Vol. 53, No. 6, June 2015

Transient Blast Response of Sandwich Plates by Dynamic Elasticity

George A. Kardomateas* and Nunthadech Rodcheuy†
Georgia Institute of Technology, Atlanta, Georgia 30332-0150
and
Yeoshua Frostig‡
Technion — Israel Institute of Technology, 32000 Haifa, Israel

DOI: 10.2514/1.J052865

The three-dimensional linear dynamic elasticity problem formulation and solution for a generally asymmetric sandwich plate consisting of core and face sheets that are orthotropic, and subjected to blast loading, is presented. Laplace transforms are used to obtain ordinary differential equations in the complex Laplace space (with the variable being the through-thickness coordinate), which are subsequently solved in closed form for a simply supported plate, with the solution involving a cubic characteristic equation with complex coefficients. Subsequently, the time response is obtained by a numerical inverse Laplace transform by use of the Euler method. A realistic material and blast case is used to demonstrate the transient behavior for the displacements and face sheet/core interfacial transverse normal and shear stresses. The elasticity results are compared with the predictions of the first-order shear deformation plate theory as well as a high-order sandwich panel theory. This dynamic elasticity solution can serve as a benchmark in assessing the accuracy of sandwich-plate theories.

Nomenclature

a	=	length of the sandwich plate
b	=	width of the sandwich plate
c	=	half-thickness of the core (total core thickness is $2c$)
c_{ij}	=	stiffness constants
E	=	axial extensional (Young's) modulus
$\tilde{F}(s)$	=	Laplace transform of $F(t)$
f_1	=	thickness of the top face
f_2	=	thickness of the bottom face
G	=	shear modulus
t	=	time
u	=	in-plane displacement (along x)
v	=	in-plane displacement (along y)
w	=	transverse displacement (along z)
γ	=	shear strain
ϵ	=	normal strain
ρ	=	mass density
σ	=	normal stress
τ	=	shear stress

Introduction

THE accurate prediction of stress and strain fields in the transient phase of response to dynamic loading is important in assuring structural integrity. In particular, when it comes to blast loading, it is generally believed that if the structure survives the first few milliseconds, then it has survived the blast. This research aims at investigating this transient phase via a dynamic elasticity approach. The configuration is a sandwich plate, consisting of two face sheets and a core, all assumed to be orthotropic in their constitutive. The general asymmetric construction is treated (i.e., face sheets may not be of the same thickness and/or material).

When a plate is subjected to an impulsive load, reflections of waves from the top and bottom surfaces as well as higher modes and short wavelength disturbances are not easily accounted for by the plate theories. Thus, these theories may not perform well even if they may be adequate for static problems or natural vibrations. Thus, an elasticity solution, being most accurate, would serve in determining the limitations of various plate theories in addressing sudden loading problems. This is also true for the various numerical methods such as the finite-element method.

For a three-dimensional sandwich plate consisting of orthotropic material, static elasticity solutions have been developed by Vlasov [1] for isotropic plates and by Pagano [2] for a restricted case of material sandwich combination. And these solutions have been extended to cover all possible orthotropic face sheet and core combinations by Kardomateas [3]. A static elasticity solution for the sandwich shell configuration has also been developed by Kardomateas [4]. Regarding the dynamic case, an elasticity solution for the free vibration of homogeneous and laminated plates was presented by Srinivas et al. [5]. Regarding the blast loading case, a sandwich beam/wide-plate elastodynamic solution has recently been developed by Kardomateas et al. [6].

The work in this paper aims at extending the sandwich beam/wide-plate elasticity formulation and solution by Kardomateas et al. [6] to the three-dimensional elasticity sandwich plate case. The sandwich plate consists of orthotropic face sheets and core and is subjected to blast loading; also, the simply supported case is considered. The formulation begins with the three-dimensional dynamic equilibrium partial differential equations. The time space is then transformed to the Laplace complex space, and the solution is obtained in closed form in the Laplace space following the solution of a cubic characteristic equation with complex coefficients. Numerical inversion to the time domain follows. The Euler numerical Laplace inversion has been selected because its accuracy has been proven for this type of problem in Kardomateas et al. [6]. Results are derived for realistic material and for blast conditions as presented in Gardner et al. [7]. The elasticity results are also compared to the first-order shear deformation plate theory.

Three-Dimensional Dynamic Elasticity Formulation

We consider a sandwich plate consisting of orthotropic face sheets of thickness f_1 and f_2 for the top and bottom, respectively, and an orthotropic core of thickness $2c$ (Fig. 1). The plate is simply supported and of length a and width b. A Cartesian coordinate system

Received 12 June 2013; accepted for publication 17 September 2013; published online 2 January 2015.

*Professor, School of Aerospace Engineering.
†Graduate Research Assistant, School of Aerospace Engineering.
‡Professor, Faculty of Civil and Environmental Engineering.

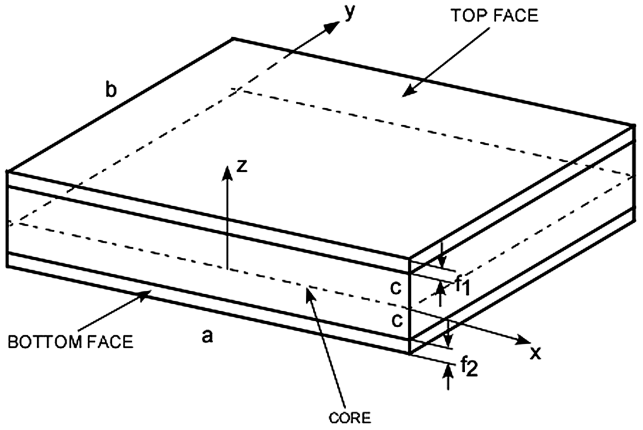

Fig. 1 Definition of the geometry for the sandwich plate.

is defined as shown in Fig. 1, with the origin being at the middle of the core.

Let us denote each phase by i, where $i = f_1$ for the upper face sheet, $i = f_2$ for the lower face sheet, and $i = c$ for the core. The displacements along x, y, and z are denoted by u, v, and w, respectively:

$$u, v, w = \text{fn}(x, y, z, t) \tag{1a}$$

Using the strain-displacement relations results in

$$\epsilon_{xx} = u_{,x}; \qquad \epsilon_{yy} = v_{,y}; \qquad \epsilon_{zz} = w_{,z} \tag{1b}$$

and

$$\gamma_{yz} = v_{,z} + w_{,y}; \qquad \gamma_{xz} = u_{,z} + w_{,x}; \qquad \gamma_{xy} = u_{,y} + v_{,x} \tag{1c}$$

The governing dynamic equilibrium equation are

$$\sigma_{xx,x} + \tau_{xy,y} + \tau_{xz,z} = \rho u_{,tt} \tag{2a}$$

$$\tau_{xy,x} + \sigma_{yy,y} + \tau_{yz,z} = \rho v_{,tt} \tag{2b}$$

$$\tau_{xz,x} + \tau_{yz,y} + \sigma_{zz,z} = \rho w_{,tt} \tag{2c}$$

For each phase i (i.e., face sheets and core), the constitutive laws for orthotropic material are

$$\begin{bmatrix} \sigma_{xx}^{(i)} \\ \sigma_{yy}^{(i)} \\ \sigma_{zz}^{(i)} \\ \tau_{yz}^{(i)} \\ \tau_{xz}^{(i)} \\ \tau_{xy}^{(i)} \end{bmatrix} = \begin{bmatrix} c_{11}^i & c_{12}^i & c_{13}^i & 0 & 0 & 0 \\ c_{12}^i & c_{22}^i & c_{23}^i & 0 & 0 & 0 \\ c_{13}^i & c_{23}^i & c_{33}^i & 0 & 0 & 0 \\ 0 & 0 & 0 & c_{44}^i & 0 & 0 \\ 0 & 0 & 0 & 0 & c_{55}^i & 0 \\ 0 & 0 & 0 & 0 & 0 & c_{66}^i \end{bmatrix} \begin{bmatrix} \epsilon_{xx}^{(i)} \\ \epsilon_{yy}^{(i)} \\ \epsilon_{zz}^{(i)} \\ \gamma_{yz}^{(i)} \\ \gamma_{xz}^{(i)} \\ \gamma_{xy}^{(i)} \end{bmatrix}, \quad (i = f_1, c, f_2) \tag{3}$$

where c_{ij}^i are the stiffness constants (where subscript ij refers to elements in the stiffness matrix).

Substituting Eqs. (1b) and (1c) into Eq. (3) results in stress-displacement relations, which when substituted into the dynamic equilibrium equations [Eq. (2)] give the following partial-differential equations for the displacements:

$$c_{11}^i u_{,xx} + c_{66}^i u_{,yy} + c_{55}^i u_{,zz} + (c_{12}^i + c_{66}^i) v_{,xy} + (c_{13}^i + c_{55}^i) w_{,xz} = \rho^i u_{,tt} \tag{4a}$$

$$(c_{12}^i + c_{66}^i) u_{,xy} + c_{66}^i v_{,xx} + c_{22}^i v_{,yy} + c_{44}^i v_{,zz} + (c_{23}^i + c_{44}^i) w_{,yz} = \rho^i v_{,tt} \tag{4b}$$

$$(c_{13}^i + c_{55}^i) u_{,xz} + (c_{23}^i + c_{44}^i) v_{,yz} + c_{55}^i w_{,xx} + c_{44}^i w_{,yy} + c_{33}^i w_{,zz} = \rho^i w_{,tt} \tag{4c}$$

In the following derivation, the superscript i shall be dropped for convenience with understanding that the derived relations hold within each phase. Appropriate displacement solutions for a simply supported plate are

$$u = U(z, t) \cos\, px \sin\, qy \tag{5a}$$

$$v = V(z, t) \sin\, px \cos\, qy \tag{5b}$$

$$w = W(z, t) \sin\, px \sin\, qy \tag{5c}$$

where

$$p = \frac{n\pi}{a}, \qquad q = \frac{m\pi}{b}, \qquad (m, n = 1, 2, 3, \ldots)$$

These assumed solutions satisfy the simply supported boundary conditions.

Then, when the assumed solutions are substituted into Eq. (4), the dynamic elasticity equilibrium equations become

$$c_{55} U_{,zz} - (c_{11} p^2 + c_{66} q^2) U - (c_{12} + c_{66}) pqV + (c_{13} + c_{55}) pW_{,z} = \rho U_{,tt} \tag{6a}$$

$$c_{44} V_{,zz} - (c_{12} + c_{66}) pqU - (c_{22} q^2 + c_{66} p^2) V + (c_{23} + c_{44}) qW_{,z} = \rho V_{,tt} \tag{6b}$$

$$c_{33} W_{,zz} - (c_{13} + c_{55}) pU_{,z} - (c_{23} + c_{44}) qV_{,z} - (c_{55} p^2 + c_{44} q^2) W = \rho W_{,tt} \tag{6c}$$

Let us denote the Laplace transform of a function $F(t)$ by $\tilde{F}(s)$, i.e.,

$$\tilde{F}(s) = \int_0^\infty F(t) e^{-st}\, \mathrm{d}t \tag{7}$$

Taking the Laplace transform of Eq. (6), and assuming zero initial displacements and velocities, results in three homogeneous ordinary differential equations for the Laplace transforms of the displacements, $\tilde{U}(z)$, $\tilde{V}(z)$, and $\tilde{W}(z)$:

$$c_{55} \tilde{U}_{,zz} - (c_{11} p^2 + c_{66} q^2 + \rho s^2) \tilde{U} - (c_{12} + c_{66}) pq\tilde{V} + (c_{13} + c_{55}) p\tilde{W}_{,z} = 0 \tag{8a}$$

$$c_{44} \tilde{V}_{,zz} - (c_{12} + c_{66}) pq\tilde{U} - (c_{66} p^2 + c_{22} q^2 + \rho s^2) \tilde{V} + (c_{23} + c_{44}) q\tilde{W}_{,z} = 0 \tag{8b}$$

$$c_{33} \tilde{W}_{,zz} - (c_{13} + c_{55}) p\tilde{U}_{,z} - (c_{23} + c_{44}) q\tilde{V}_{,z} - (c_{55} p^2 + c_{44} q^2 + \rho s^2) \tilde{W} = 0 \tag{8c}$$

Next, let us set

$$\begin{bmatrix} \tilde{U}(z) \\ \tilde{V}(z) \\ \tilde{W}(z) \end{bmatrix} = \begin{bmatrix} \tilde{U}_0 \\ \tilde{V}_0 \\ \tilde{W}_0 \end{bmatrix} e^{\lambda z} \tag{9}$$

where $\tilde{U}_0$ and $\tilde{W}_0$ are unknown constants, and substituting Eq. (9) into Eq. (8) results in the following system of algebraic equations:

$$(-c_{55}\lambda^2 + c_{11}p^2 + c_{66}q^2 + \rho s^2)\tilde{U}_0 + (c_{12} + c_{66})pq\tilde{V}_0 - (c_{13} + c_{55})p\lambda\tilde{W}_0 = 0 \tag{10a}$$

$$(c_{12} + c_{66})pq\tilde{U}_0 + (-c_{44}\lambda^2 + c_{66}p^2 + c_{22}q^2 + \rho s^2)\tilde{V}_0 - (c_{23} + c_{44})q\lambda\tilde{W}_0 = 0 \tag{10b}$$

$$(c_{13} + c_{55})p\lambda\tilde{U}_0 + (c_{23} + c_{44})q\lambda\tilde{V}_0 + (-c_{33}\lambda^2 + c_{55}p^2 + c_{44}q^2 + \rho s^2)\tilde{W}_0 = 0 \tag{10c}$$

For nontrivial solution of the system of equations, the determinant of the coefficients is zero. This results in a sixth-order polynomial equation:

$$A_0\lambda^6 + A_1\lambda^4 + A_2\lambda^2 + A_3 = 0 \tag{11a}$$

where

$$A_0 = c_{33}c_{44}c_{55} \tag{11b}$$

$$A_1 = [c_{33}c_{55}c_{66} - c_{44}(c_{13}^2 - c_{11}c_{33} + 2c_{13}c_{55})]p^2 + [c_{33}c_{44}c_{66} - c_{55}(c_{23}^2 - c_{22}c_{33} + 2c_{23}c_{44})]q^2 + + [c_{33}(c_{44} + c_{55}) + c_{44}c_{55}]\rho s^2 \tag{11c}$$

$$\begin{aligned} A_2 = {} & [2c_{12}c_{23}c_{55} - c_{12}^2c_{33} + 2c_{12}c_{44}c_{55} - 2c_{12}c_{33}c_{66} + 2c_{23}c_{55}c_{66} + 4c_{44}c_{55}c_{66} - c_{13}^2c_{22} + \\ & + 2c_{13}(c_{23} + c_{44})(c_{12} + c_{66}) - 2c_{13}c_{55}c_{22} - c_{11}c_{23}^2 + c_{11}c_{22}c_{33} - 2c_{11}c_{44}c_{23}]p^2q^2 + \\ & + (c_{22}c_{44}c_{55} - c_{23}^2c_{66} + c_{22}c_{33}c_{66} - 2c_{23}c_{44}c_{66})q^4 + (c_{11}c_{33}c_{66} + c_{11}c_{44}c_{55} - c_{13}^2c_{66} - 2c_{13}c_{55}c_{66})p^4 + \\ & + (c_{33} + c_{44} + c_{55})\rho^2s^4 + (c_{44}c_{55} + c_{33}c_{66} + c_{55}c_{66} - c_{13}^2 - 2c_{13}c_{55} + c_{11}c_{33} + c_{11}c_{44})p^2\rho s^2 + \\ & + (c_{22}c_{33} - c_{23}^2 - 2c_{23}c_{44} + c_{22}c_{55} + c_{44}c_{55} + c_{33}c_{66} + c_{44}c_{66})q^2\rho s^2 \end{aligned} \tag{11d}$$

and

$$\begin{aligned} A_3 = {} & -c_{11}c_{55}c_{66}p^6 - c_{22}c_{44}c_{66}q^6 + (c_{12}^2c_{55} - c_{11}c_{22}c_{55} - c_{11}c_{44}c_{66} + 2c_{12}c_{55}c_{66})p^4q^2 + \\ & + (c_{12}^2c_{44} - c_{11}c_{22}c_{44} + 2c_{12}c_{44}c_{66} - c_{22}c_{55}c_{66})p^2q^4 - (c_{11}c_{55} + c_{11}c_{66} + c_{55}c_{66})p^4\rho s^2 + \\ & + (c_{12}^2 - c_{11}c_{22} - c_{11}c_{44} - c_{22}c_{55} + 2c_{12}c_{66} - c_{44}c_{66} - c_{55}c_{66})p^2q^2\rho s^2 - \\ & - (c_{22}c_{44} + c_{22}c_{66} + c_{44}c_{66})q^4\rho s^2 - (c_{11} + c_{55} + c_{66})p^2\rho^2s^4 - (c_{22} + c_{44} + c_{66})q^2\rho^2s^4 - \rho^3s^6 \end{aligned} \tag{11e}$$

Let us set

$$\mu = \lambda^2 \tag{12a}$$

then Eq. (11a) is represented as a cubic polynomial equation:

$$A_0\mu^3 + A_1\mu^2 + A_2\mu + A_3 = 0 \tag{12b}$$

Equation (12b) is a cubic equation with complex coefficients. The case of a cubic equation with real coefficients is straightforward, and the corresponding explicit form for the three roots is well known. This is not the case, however, when the coefficients are complex. Instead, the roots of Eq. (12b) can be determined in closed form through a series of change of variables as follows.

The substitution

$$\mu = \rho - \frac{A_1}{3A_0} \tag{13a}$$

eliminates the μ^2 term and results in

$$\rho^3 + e\rho + f = 0 \tag{13b}$$

where

$$e = -\frac{A_1^2}{3A_0^2} + \frac{A_2}{A_0}; \qquad f = \frac{2A_1^3}{27A_0^3} - \frac{A_1A_2}{3A_0^2} + \frac{A_3}{A_0} \tag{13c}$$

Further, we proceed with the substitution (known as Vieta substitution):

$$\rho = \zeta - \frac{e}{3\zeta} \tag{13d}$$

This results in the equation

$$\zeta^6 + f\zeta^3 - \frac{e^3}{27} = 0 \tag{13e}$$

Finally, setting

$$\zeta^3 = \eta \tag{13f}$$

results in the quadratic equation with complex coefficients:

$$\eta^2 + f\eta - \frac{e^3}{27} = 0 \tag{13g}$$

In terms of the discriminant Δ of (13g), which is complex:

$$\Delta = f^2 + 4\frac{e^3}{27} \tag{13h}$$

the two complex solutions of the quadratic equation are

$$\eta_{1,2} = \frac{-f \pm \sqrt{\Delta}}{2} \tag{13i}$$

and can be set in the polar form:

$$\eta_{1,2} = r_{1,2}(\cos\theta_{1,2} + i\sin\theta_{1,2}) \tag{13j}$$

Then, from Eq. (13f) to the first root (η_1) there correspond three solutions for ζ:

$$\zeta_{1,2,3} = r_1^{1/3}\left(\cos\frac{\theta_1 + 2k\pi}{3} + i\sin\frac{\theta_1 + 2k\pi}{3}\right); \qquad k = 0, 1, 2 \tag{13k}$$

Another set of three roots correspond to the second root (η_2). Plugging back gives two sets of solutions for ρ and μ (each

corresponding to each of the two η_j), but these two sets are the same, and so finally, the three complex solutions of the cubic equation [Eq. (12b)] are

$$\mu_{1,2,3} = \zeta_{1,2,3} - \frac{e}{3\zeta_{1,2,3}} - \frac{A_1}{3A_0} \tag{13l}$$

with $\zeta_{1,2,3}$ given in Eq. (13k) for $k = 0, 1, 2$.

Therefore, from Eq. (12a), the six roots of Eq. (11a) are

$$\lambda_{1,2} = \pm\sqrt{\mu_1}, \qquad \lambda_{3,4} = \pm\sqrt{\mu_2}, \qquad \lambda_{5,6} = \pm\sqrt{\mu_3} \tag{13m}$$

Corresponding to these six roots, the general solutions (transformed displacement functions) are

$$\tilde{W}(z) = \sum_{i=1}^{6} a_i e^{\lambda_i z}; \quad \tilde{V}(z) = \sum_{i=1}^{6} b_i e^{\lambda_i z}; \quad \tilde{U}(z) = \sum_{i=1}^{6} d_i e^{\lambda_i z} \tag{14}$$

where a_i, b_i, and d_i are complex constants.

Of the 18 constants in Eq. (14), only six are independent. The remaining 12 constants can be determined in terms of the six independent constants by substituting the transformed displacements [Eq. (14)] into Eqs. (8a) and (8b). We could also select other pairs, for instance either Eqs. (8a) and (8c) or Eqs. (8b) and (8c); they both would yield the same result.

For convenience, let us set

$$f_{1i} = (c_{13} + c_{55})p\lambda_i; \qquad f_{2i} = (c_{23} + c_{44})q\lambda_i \tag{15a}$$

$$\begin{aligned} f_{3i} &= -c_{11}p^2 - c_{66}q^2 - \rho s^2 + c_{55}\lambda_i^2; \\ f_{4i} &= -c_{66}p^2 - c_{22}q^2 - \rho s^2 + c_{44}\lambda_i^2 \end{aligned} \tag{15b}$$

Then, in terms of the coefficients in the expression for $\tilde{W}(z)$, a_i we obtain

$$b_i = \frac{f_{1i}(c_{12} + c_{66})pq + f_{2i}f_{3i}}{(c_{12} + c_{66})^2 p^2 q^2 + f_{3i}f_{4i}} a_i \tag{16a}$$

$$d_i = \frac{f_{2i}(c_{12} + c_{66})pq + f_{1i}f_{4i}}{(c_{12} + c_{66})^2 p^2 q^2 - f_{3i}f_{4i}} a_i \tag{16b}$$

where $i = 1, 2, 3, 4, 5, 6$.

Thus, for each phase, there are six complex constant unknowns, which are d_i, $i = 1, \ldots 6$. The transformed displacement functions take the following form:

$$\tilde{u}(x,y,z) = \cos px \sin qy \sum_{i=1}^{6} \frac{f_{2i}(c_{12}+c_{66})pq + f_{1i}f_{4i}}{(c_{12}+c_{66})^2 p^2 q^2 - f_{3i}f_{4i}} a_i e^{\lambda_i z} \tag{17a}$$

$$\tilde{v}(x,y,z) = \sin px \cos qy \sum_{i=1}^{6} \frac{f_{1i}(c_{12}+c_{66})pq + f_{2i}f_{3i}}{(c_{12}+c_{66})^2 p^2 q^2 + f_{3i}f_{4i}} a_i e^{\lambda_i z} \tag{17b}$$

$$\tilde{w}(x,y,z) = \sin px \sin qy \sum_{i=1}^{6} a_i e^{\lambda_i z} \tag{17c}$$

The corresponding transformed stresses are derived by substituting the previous displacement expressions into Eqs. (1) and (2). We present the explicit expressions for the stresses in the following.

By setting

$$\begin{aligned} g_{ui} &= \frac{f_{2i}(c_{12} + c_{66})pq + f_{1i}f_{4i}}{(c_{12} + c_{66})^2 p^2 q^2 - f_{3i}f_{4i}}; \\ g_{vi} &= \frac{f_{1i}(c_{12} + c_{66})pq + f_{2i}f_{3i}}{(c_{12} + c_{66})^2 p^2 q^2 + f_{3i}f_{4i}} \end{aligned} \tag{18}$$

the transformed transverse normal stress $\tilde{\sigma}_{zz}(x, y, z)$ is in the form

$$\tilde{\sigma}_{zz} = \sum_{i=1}^{6} a_i b_{zzi} e^{\lambda_i z} \sin\ px \sin\ qy \tag{19a}$$

where

$$b_{zzi} = -c_{13}g_{ui}p - c_{23}g_{vi}q + c_{33}\lambda_i \tag{19b}$$

The transformed transverse shear stresses $\tilde{\tau}_{yz}(x, y, z)$ and $\tilde{\tau}_{xz}(x, y, z)$ are in the form:

$$\tilde{\tau}_{yz} = \sum_{i=1}^{6} a_i b_{yzi} e^{\lambda_i z} \sin px \cos qy; \quad \tilde{\tau}_{xz} = \sum_{i=1}^{6} a_i b_{xzi} e^{\lambda_i z} \sin px \cos qy \tag{20a}$$

where

$$b_{yzi} = c_{44}(g_{vi}\lambda_i + q); \qquad b_{xzi} = c_{55}(g_{ui}\lambda_i + p) \tag{20b}$$

The transformed axial stresses $\tilde{\sigma}_{xx}$ and $\tilde{\sigma}_{yy}$ are in the form:

$$\tilde{\sigma}_{xx} = \sum_{i=1}^{6} a_i b_{xxi} e^{\lambda_i z} \sin px \sin qy; \quad \tilde{\sigma}_{yy} = \sum_{i=1}^{6} a_i b_{yyi} e^{\lambda_i z} \sin px \sin qy \tag{21a}$$

where

$$\begin{aligned} b_{xxi} &= -c_{11}g_{ui}p - c_{12}g_{vi}q + c_{13}\lambda_i; \\ b_{yyi} &= -c_{12}g_{ui}p - c_{22}g_{vi}q + c_{23}\lambda_i \end{aligned} \tag{21b}$$

Finally there is an in-plane shear stress $\tilde{\tau}_{xy}(x, y, z)$ in the form:

$$\tilde{\tau}_{xy} = \sum_{i=1}^{6} a_i b_{xyi} e^{\lambda_i z} \cos\ px \cos\ qy \tag{22a}$$

where

$$b_{xyi} = c_{66}(qg_{ui} + pg_{vi}) \tag{22b}$$

From this analysis, we can see that, within each phase (i), where $i = f_1, c, f_2$, there are six constants: $a_j^{(i)}$, $j = 1, \ldots 6$. Therefore, for the three phases, this gives a total of 18 constants to be determined.

These 18 constants are determined from the conditions on the bounding surfaces and the face sheet/core interfaces as follows.

There are three traction conditions at the lower face-sheet/core interface, $z = -c$.

Condition 1: $\tilde{\sigma}_{zz}^{(c)} = \tilde{\sigma}_{zz}^{(f2)}$ at $z = -c$, which gives

$$\sum_{j=1}^{6} b_{zzj}^{(c)} e^{-c\lambda_j^{(c)}} a_j^{(c)} = \sum_{j=1}^{6} b_{zzj}^{(f2)} e^{-c\lambda_j^{(f2)}} a_j^{(f2)} \tag{23a}$$

Condition 2: $\tilde{\tau}_{xz}^{(c)} = \tilde{\tau}_{xz}^{(f2)}$ at $z = -c$, which gives

$$\sum_{j=1}^{6} b_{xzj}^{(c)} e^{-c\lambda_j^{(c)}} a_j^{(c)} = \sum_{j=1}^{6} b_{xzj}^{(f2)} e^{-c\lambda_j^{(f2)}} a_j^{(f2)} \tag{23b}$$

Condition 3: $\tilde{\tau}_{yz}^{(c)} = \tilde{\tau}_{yz}^{(f2)}$ at $z = -c$, which gives

$$\sum_{j=1}^{6} b_{yzj}^{(c)} e^{-c\lambda_j^{(c)}} a_j^{(c)} = \sum_{j=1}^{6} b_{yzj}^{(f2)} e^{-c\lambda_j^{(f2)}} a_j^{(f2)} \tag{23c}$$

There are also three displacement continuity conditions at the lower core/face-sheet interfaces.

Condition 4: $\tilde{U}^{(c)} = \tilde{U}^{(f2)}$ at $z = -c$, which results in

$$\sum_{j=1}^{6} g_{uj}^{(c)} e^{-c\lambda_j^{(c)}} a_j^{(c)} = \sum_{j=1}^{6} g_{uj}^{(f2)} e^{-c\lambda_j^{(f2)}} a_j^{(f2)} \tag{23d}$$

Condition 5: $\tilde{V}^{(c)} = \tilde{V}^{(f2)}$ at $z = -c$, which results in

$$\sum_{j=1}^{6} g_{vj}^{(c)} e^{-c\lambda_j^{(c)}} a_j^{(c)} = \sum_{j=1}^{6} g_{vj}^{(f2)} e^{-c\lambda_j^{(f2)}} a_j^{(f2)} \tag{23e}$$

Condition 6: $\tilde{W}^{(c)} = \tilde{W}^{(f2)}$ at $z = -c$, which gives

$$\sum_{j=1}^{6} e^{-c\lambda_j^{(c)}} a_j^{(c)} = \sum_{j=1}^{6} e^{-c\lambda_j^{(f2)}} a_j^{(f2)} \tag{23f}$$

Next, there are three traction conditions at the upper face-sheet/core interface, $z = +c$.

Condition 7: $\tilde{\sigma}_{zz}^{(f1)} = \tilde{\sigma}_{zz}^{(c)}$ at $z = +c$, which gives

$$\sum_{j=1}^{6} b_{zzj}^{(c)} e^{c\lambda_j^{(c)}} a_j^{(c)} = \sum_{j=1}^{6} b_{zzj}^{(f1)} e^{c\lambda_j^{(f1)}} a_j^{(f1)} \tag{24a}$$

Condition 8: $\tilde{\tau}_{xz}^{(f1)} = \tilde{\tau}_{xz}^{(c)}$ at $z = +c$, which gives

$$\sum_{j=1}^{6} b_{xzj}^{(c)} e^{c\lambda_j^{(c)}} a_j^{(c)} = \sum_{j=1}^{6} b_{xzj}^{(f1)} e^{c\lambda_j^{(f1)}} a_j^{(f1)} \tag{24b}$$

Condition 9: $\tilde{\tau}_{yz}^{(c)} = \tilde{\tau}_{yz}^{(f1)}$ at $z = +c$, which gives

$$\sum_{j=1}^{6} b_{yzj}^{(c)} e^{c\lambda_j^{(c)}} a_j^{(c)} = \sum_{j=1}^{6} b_{yzj}^{(f1)} e^{c\lambda_j^{(f1)}} a_j^{(f1)} \tag{24c}$$

The corresponding displacement continuity conditions at the upper face-sheet/core interface, $z = +c$ are as follows.

Condition 10: $\tilde{U}^{(f1)} = \tilde{U}^{(c)}$ at $z = +c$, which gives

$$\sum_{j=1}^{6} g_{uj}^{(c)} e^{c\lambda_j^{(c)}} a_j^{(c)} = \sum_{j=1}^{6} g_{uj}^{(f1)} e^{c\lambda_j^{(f1)}} a_j^{(f1)} \tag{24d}$$

Condition 11: $\tilde{V}^{(c)} = \tilde{V}^{(f1)}$ at $z = +c$, which results in

$$\sum_{j=1}^{6} g_{vj}^{(c)} e^{c\lambda_j^{(c)}} a_j^{(c)} = \sum_{j=1}^{6} g_{vj}^{(f1)} e^{c\lambda_j^{(f1)}} a_j^{(f1)} \tag{24e}$$

Condition 12: $\tilde{W}^{(f1)} = \tilde{W}^{(c)}$ at $z = +c$, which gives

$$\sum_{j=1}^{6} e^{c\lambda_j^{(c)}} a_j^{(c)} = \sum_{j=1}^{6} e^{c\lambda_j^{(f1)}} a_j^{(f1)} \tag{24f}$$

Finally, two traction conditions exist on each of the two bounding surfaces. The traction free conditions at the lower bounding surface, $z = -(c + f_2)$, can be written as follows.

Condition 13: $\tilde{\sigma}_{zz} = 0$ at $z = -(c + f2)$, which gives

$$\sum_{j=1}^{6} b_{zzj}^{(f2)} e^{-(c+f_2)\lambda_j^{(f2)}} a_j^{(f2)} = 0 \tag{25a}$$

Condition 14: $\tilde{\tau}_{xz} = 0$ at $z = -(c + f2)$, which gives

$$\sum_{j=1}^{6} b_{xzj}^{(f2)} e^{-(c+f_2)\lambda_j^{(f2)}} a_j^{(f2)} = 0 \tag{25b}$$

Condition 15: $\tilde{\tau}_{yz} = 0$ at $z = -(c + f2)$, which gives

$$\sum_{j=1}^{6} b_{yzj}^{(f2)} e^{-(c+f_2)\lambda_j^{(f2)}} a_j^{(f2)} = 0 \tag{25c}$$

We assume that a transverse distributed loading $q_0(x, y, t)$ per unit width is applied at the top face sheet. If the form of the distributed load is

$$q_0(x, y, t) = Q_0(t) \sin\frac{n\pi x}{a} \sin\frac{m\pi y}{b} = Q_0(t) \sin\ px\ \sin\ qy \tag{26}$$

and the Laplace transform of $Q_0(t)$ is $\tilde{Q}_0(s)$, then at the upper bounding surface, where the transverse load $q_0(x, y, t)$ is applied, we have the condition:

Condition 16: $\tilde{\sigma}_{zz}|_{z=(c+f1)} = \tilde{Q}_0(s) \sin\ px\ \sin\ qy$, which gives

$$\sum_{j=1}^{6} b_{zzj}^{(f1)} e^{(c+f_1)\lambda_j^{(f1)}} a_j^{(f1)} = \tilde{Q}_0(s) \tag{27a}$$

For example, for an exponential decay loading $Q_0(t) = A_0 e^{-t/c}$, we would have $\tilde{Q}_0(s) = A_0 c/(1 + sc)$. For a pulse loading of amplitude A_0 and of infinite duration, $Q_0(t) = A_0 H(t)$, where H is the Heaviside unit function, we would have $\tilde{Q}_0(s) = A_0/s$, and for a pulse loading of amplitude A_0 and of finite duration t_0, we would have $\tilde{Q}_0(s) = A_0(1 - e^{-t_0 s})/s$.

Moreover, we have the second traction condition at the bounding surface of the top face sheet.

Condition 17: $\tilde{\tau}_{xz}|_{z=(c+f1)} = 0$, which gives

$$\sum_{i=1}^{6} b_{xzj}^{(f1)} e^{(c+f_1)\lambda_j^{(f1)}} a_j^{(f1)} = 0 \tag{27b}$$

and the third traction condition at the bounding surface of the top face sheet

Condition 18: $\tilde{\tau}_{yz}|_{z=(c+f1)} = 0$, which gives

$$\sum_{i=1}^{6} b_{yzj}^{(f1)} e^{(c+f_1)\lambda_j^{(f1)}} a_j^{(f1)} = 0 \tag{27c}$$

Therefore, we have a system of 18 linear algebraic equations in the 18 (in general complex) unknowns, $a_j^{(f2)}$, $a_j^{(c)}$, and $a_j^{(f1)}$, $j = 1, 6$. Solving for these determines in closed form the Laplace transforms of the displacement and stress fields.

The next step is the inversion back to the time space, which is done numerically. This a critical part of this research because there exist many approaches to numerical inversion of Laplace transforms [8], and each method is suitable for certain physical problems; for example, different methods would be needed for heat transfer problems as opposed to structural vibration problems. The Euler

method, as described in Abate and Whitt [9], was found to provide excellent accuracy by comparing its application to the closed-form classical beam-theory vibration equations of a simple homogeneous beam of the same overall stiffness as our sandwich beam. As discussed also in [3], the numerical inversion based on the Euler method produced results in the time space that were exactly the theoretical results up to a time of about 10 ms.

The Euler method, so named because it employs Euler summation, is based on the Bromwich contour inversion integral, which can be expressed as the integral of a real-valued function of a real variable by choosing a specific contour [6]. The integral is calculated by use of the Fourier-series method (the Poisson summation formula) and the Euler summation to accelerate convergence. In addition to confirming the numerical inversion by comparing to the closed-form simple vibration equation, the accuracy was further confirmed in the time scale of interest by comparing with the results from the Post–Widder method, again described in [9]. It should be noticed that both the Euler and the Post–Widder methods are variants of the Fourier-series method but are dramatically different so that they can be expected to serve as useful checks on each other.

First-Order Shear Sandwich-Plate Theory

Let us denote by $\psi_1(x, y, t)$ and $\psi_2(x, y, t)$ the rotations of the cross sections originally perpendicular to the x and y axes, respectively, and $w(x, y, t)$ the transverse deflection (i.e., along the z axis and taken as one for the entire section). The plate is loaded with a transverse load $q_0(x, y, t)$. Based on the assumptions of the theory, the displacements are assumed in the form:

$$u(x, y, z, t) = u_0(x, y, t) + z\psi_1(x, y, t) \tag{28a}$$

$$v(x, y, z, t) = v_0(x, y, t) + z\psi_2(x, y, t) \tag{28b}$$

$$w(x, y, z, t) = w_0(x, y, t) \tag{28c}$$

The static first-order shear deformation (FOSD) theory equations for a sandwich plate can be found in Carlsson and Kardomateas [10] and can be directly extended to the dynamic case following the general dynamic plate equations in Birman [11].

For the transverse displacement and shear functions, these are

$$D_{11}\psi_{1,xx} + (D_{12} + D_{66})\psi_{2,xy} + D_{66}\psi_{1,yy} - \kappa D_{55}(\psi_1 + w_{0,x}) = (\rho I)_{\text{eq}}\frac{\partial^2\psi_1}{\partial t^2} \tag{29a}$$

$$D_{22}\psi_{2,yy} + (D_{12} + D_{66})\psi_{1,xy} + D_{66}\psi_{2,xx} - \kappa D_{44}(\psi_2 + w_{0,y}) = (\rho I)_{\text{eq}}\frac{\partial^2\psi_2}{\partial t^2} \tag{29b}$$

$$\kappa D_{55}(\psi_{1,x} + w_{0,xx}) + \kappa D_{44}(\psi_{2,y} + w_{0,yy}) + q(x, y, t) = (\rho h)_{\text{eq}}\frac{\partial^2 w_0}{\partial t^2} \tag{29c}$$

We shall present results in the next section for a symmetric sandwich; thus, we assume a symmetric construction that would simplify the relations, and in this case $E^t_{1,2} = E^b_{1,2} = E^f_{1,2}$ and $f_1 = f_2 = f$ and the densities $\rho_t = \rho_b = \rho_f$.

Therefore, the bending rigidities about the y and x axes per unit width, D_{11}, D_{22}, respectively, are

$$D_{jj} = 2\left[E^f_j\frac{f^3}{12} + E^f_j f\left(\frac{f}{2} + c\right)^2\right] + E^c_j\frac{(2c)^3}{12}; \qquad j = 1, 2 \tag{30a}$$

The rigidity associated with the in-plane shear (twisting rigidity) is

$$D_{66} = 2\left[G^f_{12}\frac{f^3}{12} + G^f_{12}f\left(\frac{f}{2} + c\right)^2\right] + G^c_{12}\frac{(2c)^3}{12}; \qquad j = 1, 2 \tag{30b}$$

In the most-followed version of this theory, the contribution of the core is neglected in Eqs. (30a) and (30b) [10], but we include it here to bring it closer to the elasticity theory assumptions.

In addition, because the core is assumed to be the only contributor to the transverse shear, the rigidity constants associated with the transverse shear are

$$D_{55} = G^c_{13}(2c); \qquad D_{44} = G^c_{23}(2c) \tag{30c}$$

Although the shear correction factor in homogeneous sections is taken typically as $\kappa = 5/6$, in a sandwich section the shear stress distribution in the core is largely uniform, and therefore we set $\kappa = 1$ as the shear correction factor.

Furthermore, $(\rho h)_{\text{eq}}$ is defined from the densities and thicknesses of the faces and the core as

$$(\rho h)_{\text{eq}} = 2\rho_f f + \rho_c(2c) \tag{30d}$$

and $(\rho I)_{\text{eq}}$ is defined from the densities and the moments of inertia of the faces and the core with respect to the neutral axis for the sandwich section as

$$(\rho I)_{\text{eq}} = 2\rho_f\left[\frac{f^3}{12} + f\left(\frac{f}{2} + c\right)^2\right] + \rho_c\left[\frac{(2c)^3}{12} + (2c)e^2\right] \tag{30e}$$

Setting

$$w_0(x, y, t) = W_0(t)\sin\ px\ \sin\ qx \tag{31a}$$

$$\psi_1(x, y, t) = \Psi_1(t)\cos\ px\ \sin\ qy \tag{31b}$$

$$\psi_2(x, y, t) = \Psi_2(t)\sin\ px\ \cos\ qy \tag{31c}$$

with $p = n\pi/a$ and $q = m\pi/b$ and with the load in the same manner as Eq. (26), and substituting in Eqs. (29a–29c) leads to

$$-D_{11}p^2\Psi_1(t) - (D_{12} + D_{66})pq\Psi_2(t) - D_{66}q^2\Psi_1(t) - \kappa D_{55}[\Psi_1(t) + pW_0(t)] = (\rho I)_{\text{eq}}\frac{\mathrm{d}^2\Psi_1(t)}{\mathrm{d}t^2} \tag{32a}$$

$$-D_{22}q^2\Psi_2(t) - (D_{12} + D_{66})pq\Psi_1(t) - D_{66}p^2\Psi_2(t) - \kappa D_{44}[\Psi_2(t) + qW_0(t)] = (\rho I)_{\text{eq}}\frac{\mathrm{d}^2\Psi_2(t)}{\mathrm{d}t^2} \tag{32b}$$

$$-\kappa D_{55}[p\Psi_1(t) + p^2W_0(t)] - \kappa D_{44}[q\Psi_2(t) + q^2W_0(t)] + Q_0(t) = (\rho h)_{\text{eq}}\frac{\mathrm{d}^2W_0(t)}{\mathrm{d}t^2} \tag{32c}$$

Taking the Laplace transforms of the foregoing equations gives

$$[(\rho I)_{\text{eq}}s^2 + D_{11}p^2 + D_{66}q^2 + \kappa D_{55}]\tilde{\Psi}_1 + (D_{12} + D_{66})pq\tilde{\Psi}_2 + \kappa D_{55}p\tilde{W}_0 = 0 \tag{33a}$$

$$(D_{12} + D_{66})pq\tilde{\Psi}_1 + [(\rho I)_{\text{eq}}s^2 + D_{22}q^2 + D_{66}p^2 + \kappa D_{44}]\tilde{\Psi}_2 + \kappa D_{44}q\tilde{W}_0 = 0 \tag{33b}$$

$$\kappa D_{55} p\tilde{\Psi}_1 + \kappa D_{44} q\tilde{\Psi}_2 + [(\rho h)_{\text{eq}} s^2 + \kappa D_{55} p^2 + \kappa D_{44} q^2]\tilde{W}_0 = \tilde{Q}_0 \tag{33c}$$

Thus, we have three algebraic equations in three unknowns, $\tilde{\Psi}_1$, $\tilde{\Psi}_2$, and $\tilde{W}_0$, and these can be solved in closed form in the Laplace space.

In particular, in terms of the determinant:

$$D = \begin{bmatrix} (\rho I)_{\text{eq}} s^2 + D_{11} p^2 + D_{66} q^2 + \kappa D_{55} & (D_{12} + D_{66}) pq & \kappa D_{55} p \\ (D_{12} + D_{66}) pq & (\rho I)_{\text{eq}} s^2 + D_{22} q^2 + D_{66} p^2 + \kappa D_{44} & \kappa D_{44} q \\ \kappa D_{55} p & \kappa D_{44} q & (\rho h)_{\text{eq}} s^2 + \kappa D_{55} p^2 + \kappa D_{44} q^2 \end{bmatrix} \tag{34a}$$

the solution is

$$\tilde{\Psi}_1 = p\kappa\tilde{Q}_0 \frac{D_{44}(D_{12} + D_{66})q^2 - D_{55}[(\rho I)_{\text{eq}} s^2 + q^2 D_{22} + p^2 D_{66} + \kappa D_{44}]}{D} \tag{34b}$$

$$\tilde{\Psi}_2 = q\kappa\tilde{Q}_0 \frac{D_{55}(D_{12} + D_{66})p^2 - D_{44}[(\rho I)_{\text{eq}} s^2 + p^2 D_{11} + q^2 D_{66} + \kappa D_{55}]}{D} \tag{34c}$$

and

$$\tilde{W}_0 = \tilde{Q}_0 \frac{[(\rho I)_{\text{eq}} s^2 + p^2 D_{11} + q^2 D_{66} + \kappa D_{55}][(\rho I)_{\text{eq}} s^2 + q^2 D_{22} + p^2 D_{66} + \kappa D_{44}] - p^2 q^2 (D_{12} + D_{66})^2}{D} \tag{34d}$$

Notice that this theory would predict no normal strains ($e_{zz} = 0$) and shear stresses in the core that have no z variation and are of the form:

$$\tau_{xz} = G^c_{13}(\psi_1 + w_{0,x}); \qquad \tau_{yz} = G^c_{23}(\psi_2 + w_{0,y}) \tag{34e}$$

The inversion of the previous equation is implemented in the same way as for the elasticity (i.e., the Euler method, as described in [9]).

Results and Discussion

The material used in the calculations is based on the experiments of Gardner et al. [7]. Both top and bottom face sheets are made from glass vinyl ester with $E^f_1 = E^f_2 = E^f_3 = 13.6$ GPa; $G^f_{23} = G^f_{13} = G^f_{12} = 5.2$ GPa; $\nu^f_{12} = \nu^f_{13} = 0.25$ and $\nu^f_{32} = 0.35$ and density $\rho_f = 1800$ kg/m^3. The core is made from Corecell foam with $E^c_1 = E^c_2 = E^c_3 = 0.032$ GPa; $G^c_{23} = G^c_{13} = G^c_{12} = 0.020$ GPa; $\nu^c_{12} = \nu^c_{13} = 0.25$ and $\nu^c_{32} = 0.35$ and density $\rho_c = 58.5$ kg/m^3. The sandwich plate is symmetric with face thickness $f = 5$ mm, core thickness $2c = 38$ mm, length $a = 152.4$ mm, and width $b = 102$ mm.

For the sake of simplicity, we assume single half-wave sinusoidal loadings in x and y, i.e., in Eq. (26), $n = 1$ and $m = 1$. Note that a general loading can be expanded in a series of terms of the type of Eq. (26) anyway.

The time dependence of the loading is constructed from the shock-wave history reported in Gardner et al. [7] and is expressed in the form of an exponentially decaying blast:

$$Q_0(t) = -0.51e^{-1.25t} \text{ GN/m}^2 \tag{35a}$$

where t is given in seconds.

Thus, the Laplace transform of the load is

$$\tilde{Q}_0(s) = -0.51/(s + 1.25) \tag{35b}$$

For each phase (top and bottom face sheet and core), the stiffness constants c_{ij} that enter into the elasticity solution are found from

$$c_{11} = E_1 \frac{(1 - \nu_{23}\nu_{32})}{C_0}; \qquad c_{12} = E_2 \frac{(\nu_{12} + \nu_{13}\nu_{32})}{C_0}; \qquad c_{13} = E_3 \frac{(\nu_{13} + \nu_{12}\nu_{23})}{C_0} \tag{36a}$$

$$c_{22} = E_2 \frac{(1 - \nu_{13}\nu_{31})}{C_0}; \qquad c_{23} = E_3 \frac{(\nu_{23} + \nu_{21}\nu_{13})}{C_0}; \qquad c_{33} = E_3 \frac{(1 - \nu_{12}\nu_{21})}{C_0} \tag{36b}$$

$$c_{44} = G_{23}; \qquad c_{55} = G_{31}; \qquad c_{66} = G_{12} \tag{36c}$$

where

$$C_0 = 1 - (\nu_{12}\nu_{21} + \nu_{23}\nu_{32} + \nu_{13}\nu_{31}) - (\nu_{12}\nu_{23}\nu_{31} + \nu_{21}\nu_{13}\nu_{32}) \tag{36d}$$

Plotted in Fig. 2a is the transverse displacement w of the midtop face, midcore, and midbottom face, at plate center, $x = a/2$, $y = b/2$, as a function of time during the first millisecond. It can be seen that the bottom face is lagging the top face, whereas the core is also following a different path. At about 0.20 ms, it can be seen that the top face is displacing by about 4 mm more than the bottom face; thus, the core is substantially compressed. Beyond about 0.35 ms, the bottom face starts displacing more than the top face, which means that the core is expanding, but this expansion is of smaller scale than the core compression, with the maximum being about 1 mm. At about 0.48 ms, the core compression resumes. Notice also that the displacements are of the same scale as the measured ones in Wang and Shukla [12].

The commonly used first-order shear deformation (FOSD) theory predictions are shown in Fig. 2b. It can be seem that the FOSD theory cannot capture the divergences and lag behavior between faces and core because it is in terms of only one transverse displacement for the entire structure and that the FOSD theory significantly overestimates the dynamic displacements; in fact, the peaks and troughs of the FOSD are about 50% over the corresponding ones from elasticity. Although the FOSD is not adequate, high-order theories are expected to be more accurate. In fact, the extended high-order sandwich-panel theory (EHSAPT) recently developed by Phan et al. [13] was proven to be very accurate in its static-beam version [13] and in its dynamic-beam version [14]. This theory was extended to its dynamic plate version [15] and is compared to the elasticity results in Fig. 2b. It can

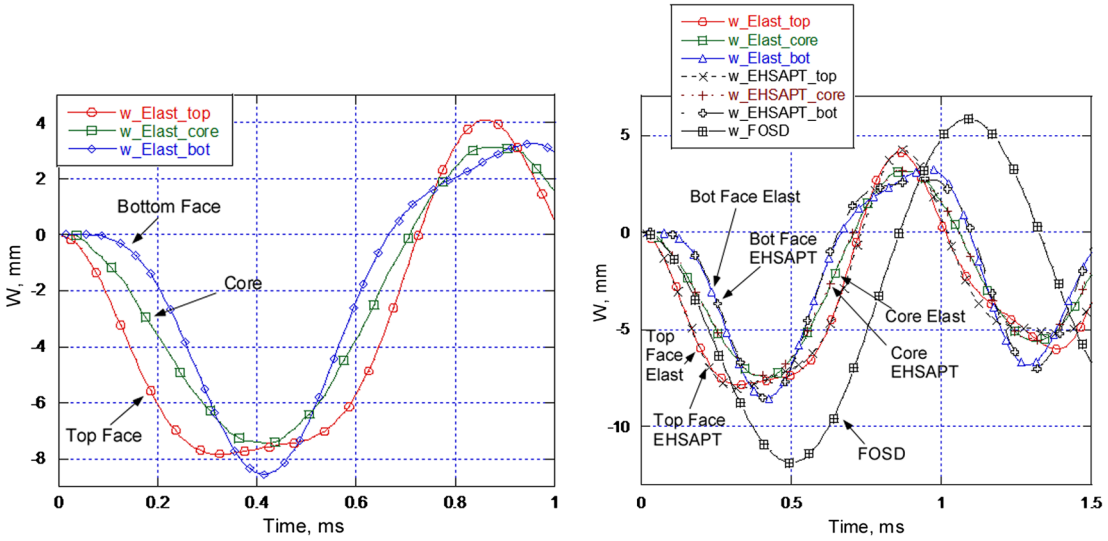

a) b)

Fig. 2 Transverse displacement w of a) face sheets and midcore during the first millisecond, and b) from FOSD and EHSAPT vs elasticity.

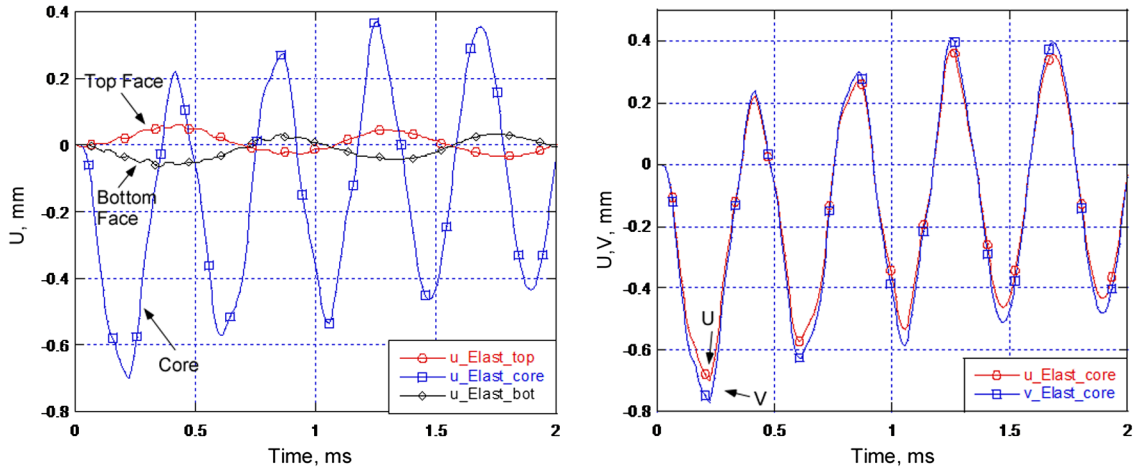

a) b)

Fig. 3 Representations (during the first 2 ms) of a) axial displacement u at the middle of the faces and the core, and b) axial displacements u and v at the middle of the core.

be observed that the EHSAPT is very accurate and on top of the elasticity and can capture very well the differing behaviors of the face sheets and the core.

Figure 3a shows the axial displacement u of the midtop face, midbottom face, and midcore at $x = a/4$ and $y = b/4$ as a function of time during the first 2 ms. The core experiences higher axial displacement and cyclic behavior in comparison with the top and bottom sheets. It can also be observed that the two face sheets displace in an opposing manner.

Figure 3b compares the two axial displacements u and v at the middle of the core, and it can be seen that they show only small differences in magnitude and follow the same cyclic behavior.

Figure 4 shows the transverse normal stress at the top face/core interface and the bottom face/core interface at the plate center, $x = a/2$ and $y = b/2$, as a function of time during the first 2 ms. Both the top and bottom interfaces encounter compression and tension alternatively. The maximum compressive stress of 0.58 MPa is at the top interface and occurs at 0.22 ms, and the maximum tensile stress of 0.34 MPa is at the bottom interface and occurs at 1.65 ms. Furthermore, it can be observed that the top interface is mostly in compression, whereas the bottom interface undergoes fairly evenly tension and compression. It can also be seen that the interfacial normal stress σ_{zz} follows the cyclic behavior of the core axial displacements.

Figure 5 shows the shear stress τ_{xz} at the top and bottom face sheet-core interfaces at quarter-distance, $x = a/4$, $y = b/4$. We observe that the shear stress follows the same cyclic behavior as the transverse

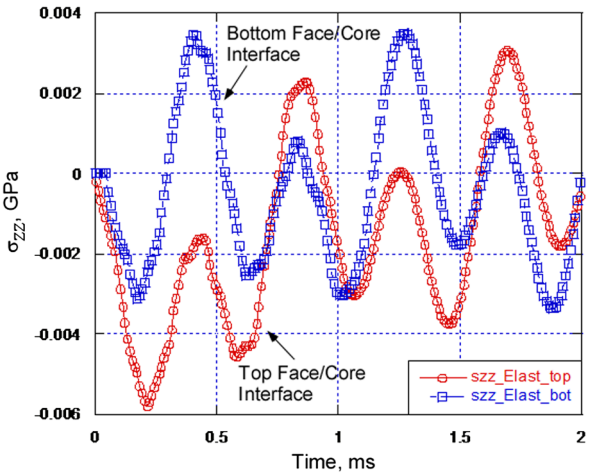

Fig. 4 Transverse normal stress σ_{zz} at the face/core interfaces during the initial phase of blast.

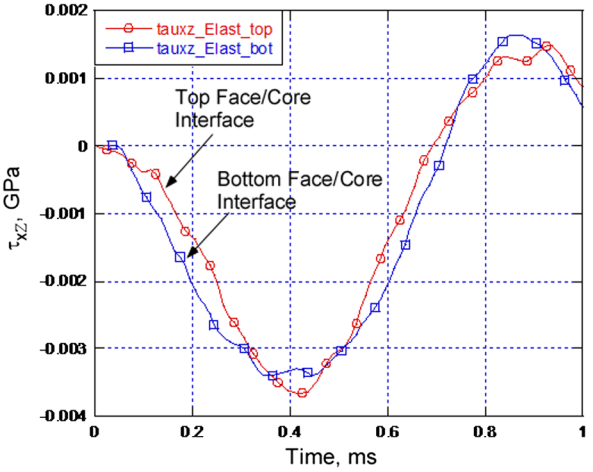

Fig. 5 Shear stress τ_{xz} at the face/core interfaces during the first millisecond.

displacement (Fig. 2a). The shear stress is, in general, higher for the bottom face/core interface and peaks at about 0.45 ms. It switches sign at about 0.70 ms. The peak transverse shear stress is comparable in magnitude to the peak tensile transverse normal (Fig. 4). Similar trends and values hold for the other transverse shear τ_{yz}. The magnitude of the shear stress at the interfaces is considerable, and given the fact that inside the core there would be shear stresses of similar magnitude, it can explain the core cracking initiating at about 0.5 ms, which was observed in experiments [7].

Conclusions

A dynamic three-dimensional elasticity solution for the transient response of a sandwich plate consisting of orthotropic core and face sheets and subjected to blast loading at the top face sheet was presented. The problem was formulated with the three-dimensional dynamic equilibrium equations in time domain, which are then transformed to the Laplace domain. Subsequently, the Laplace domain solutions are obtained in closed form, with the solution involving a cubic characteristic equation with complex coefficients. The Laplace domain solutions are numerically inverted back to the time domain by use of the Euler method, which is based on the Bromwich contour inversion integral. The results for a certain realistic case were produced and showed that the sandwich structure exhibits a cyclic displacement response with appreciable lags and leads between top and bottom face sheet and core. Moreover, the structure exhibits both transverse normal compression and tension at the face/core interfaces, with the normal compression stress dominating the top interface and the bottom interface showing fair amounts of both. Finally, the interfacial shear stresses also showed a remarkable magnitude and the same cyclic behavior as the transverse displacement. This elasticity solution can be used as a benchmark in assessing the accuracy of the various sandwich-plate theories.

Acknowledgments

The financial support of the Office of Naval Research, grant N00014-11-1-0597, and the interest and encouragement of the Grant Monitor, Y. D. S. Rajapakse, are both gratefully acknowledged.

References

[1] Vlasov, B. F., "On One Case of Bending of Rectangular Thick Plates," Vestnik Moskovskogo Universiteta. Serieii'a Matematiki, Mekhaniki, Astronomii, Fiziki, Khimii, No. 2, 1957, pp. 25–34 (in Russian).

[2] Pagano, N. J., "Exact Solutions for Rectangular Bidirectional Composites and Sandwich Plates," *Journal of Composite Materials*, Vol. 4, No. 1, 1970, pp. 20–34.

[3] Kardomateas, G. A., "Three Dimensional Elasticity Solution for Sandwich Plates with Orthotropic Phases: the Positive Discriminant Case," *Journal of Applied Mechanics*, Vol. 76, No. 1, 2009, Paper 014505. doi:10.1115/1.2966174

[4] Kardomateas, G. A., "Elasticity Solutions for a Sandwich Orthotropic Cylindrical Shell Under External Pressure, Internal Pressure and Axial Force," *AIAA Journal*, Vol. 39, No. 4, April 2001, pp. 713–719. doi:10.2514/2.1366

[5] Srinivas, S., Joga Rao, C. V., and Rao, A. K., "An Exact Analysis for Vibration of Simply-Supported Homogeneous and Laminated Thick Rectangular Plates," *Journal of Sound and Vibration*, Vol. 12, No. 2, 1970, pp. 187–199. doi:10.1016/0022-460X(70)90089-1

[6] Kardomateas, G. A., Frostig, Y., and Phan, C. N., "Dynamic Elasticity Solution for the Transient Blast Response of Sandwich Beams/Wide Plates," *AIAA Journal*, Vol. 51, No. 2, 2013, pp. 485–491. doi:10.2514/1.J051885

[7] Gardner, N., Wang, E., Kumar, P., and Shukla, A., "Blast Mitigation in a Sandwich Composite Using Graded Core and Polyurea Interlayer," *Experimental Mechanics*, Vol. 52, No. 2, Feb. 2012, pp. 119–133. doi:10.1007/s11340-011-9517-9

[8] Cohen, A. M., *Numerical Methods for Laplace Transform Inversion*, Springer–Verlag, New York, 2007.

[9] Abate, J., and Whitt, W., "Numerical Inversion of Laplace Transforms of Probability Distributions," *ORSA Journal on Computing*, Vol. 7, No. 1, 1995, pp. 36–43. doi:10.1287/ijoc.7.1.36

[10] Carlsson, L., and Kardomateas, G. A., *Structural and Failure Mechanics of Sandwich Composites*, Springer, New York, 2011.

[11] Birman, V., *Plate Structures*, Springer, New York, 2011.

[12] Wang, E., and Shukla, A., "Blast Performance of Sandwich Composites with In-Plane Compressive Loading," *Experimental Mechanics*, Vol. 52, No. 1, Jan. 2012, pp. 49–58. doi:10.1007/s11340-011-9500-5

[13] Phan, C. N., Frostig, Y., and Karomateas, G. A., "Analysis of Sandwich Panels with a Compliant Core and with In-Plane Rigidity-Extended High-Order Sandwich Panel Theory Versus Elasticity," *Journal of Applied Mechanics*, Vol. 79, No. 4, 2012, Paper 041001. doi:10.1115/1.4005550

[14] Phan, C. N., Kardomateas, G. A., and Frostig, Y., "Blast Response of a Sandwich Beam/Wide Plate Based on the Extended High-Order Sandwich Panel Theory (EHSAPT) and Comparison with Elasticity," *Journal of Applied Mechanics*, Vol. 80, No. 6, Aug. 2013, Paper 061005. doi:10.1115/1.4023619

[15] Frostig, Y., Rodcheuy, N., and Kardomateas, G. A., "Blast Response of Sandwich Plates with a Compressible Core-Extended High-Order Sandwich Panel Approach," *AIAA Journal*, 2014 (in press).

S. Pellegrino
Associate Editor